Observation of direct *CP* violation in the measurement of the Cabibbo-Kobayashi-Maskawa angle γ with $B^{\pm} \rightarrow D^{(*)}K^{(*)\pm}$ decays

J. P. Lees,[1] V. Poireau,[1] V. Tisserand,[1] E. Grauges,[2] A. Palano,[3a,3b] G. Eigen,[4] B. Stugu,[4] D. N. Brown,[5] L. T. Kerth,[5] Yu. G. Kolomensky,[5] G. Lynch,[5] H. Koch,[6] T. Schroeder,[6] D. J. Asgeirsson,[7] C. Hearty,[7] T. S. Mattison,[7] J. A. McKenna,[7] R. Y. So,[7] A. Khan,[8] V. E. Blinov,[9] A. R. Buzykaev,[9] V. P. Druzhinin,[9] V. B. Golubev,[9] E. A. Kravchenko,[9] A. P. Onuchin,[9] S. I. Serednyakov,[9] Yu. I. Skovpen,[9] E. P. Solodov,[9] K. Yu. Todyshev,[9] A. N. Yushkov,[9] D. Kirkby,[10] A. J. Lankford,[10] M. Mandelkern,[10] H. Atmacan,[11] J. W. Gary,[11] O. Long,[11] G. M. Vitug,[11] C. Campagnari,[12] T. M. Hong,[12] D. Kovalskyi,[12] J. D. Richman,[12] C. A. West,[12] A. M. Eisner,[13] J. Kroseberg,[13] W. S. Lockman,[13] A. J. Martinez,[13] B. A. Schumm,[13] A. Seiden,[13] D. S. Chao,[14] C. H. Cheng,[14] B. Echenard,[14] K. T. Flood,[14] D. G. Hitlin,[14] P. Ongmongkolkul,[14] F. C. Porter,[14] A. Y. Rakitin,[14] R. Andreassen,[15] Z. Huard,[15] B. T. Meadows,[15] M. D. Sokoloff,[15] L. Sun,[15] P. C. Bloom,[16] W. T. Ford,[16] A. Gaz,[16] U. Nauenberg,[16] J. G. Smith,[16] S. R. Wagner,[16] R. Ayad,[17,*] W. H. Toki,[17] T. M. Karbach,[18,†] B. Spaan,[18] K. R. Schubert,[19] R. Schwierz,[19] D. Bernard,[20] M. Verderi,[20] P. J. Clark,[21] S. Playfer,[21] D. Bettoni,[22a] C. Bozzi,[22a] R. Calabrese,[22a,22b] G. Cibinetto,[22a,22b] E. Fioravanti,[22a,22b] I. Garzia,[22a,22b] E. Luppi,[22a,22b] L. Piemontese,[22a] V. Santoro,[22a] R. Baldini-Ferroli,[23] A. Calcaterra,[23] R. de Sangro,[23] G. Finocchiaro,[23] P. Patteri,[23] I. M. Peruzzi,[23,‡] M. Piccolo,[23] M. Rama,[23] A. Zallo,[23] R. Contri,[24a,24b] E. Guido,[24a,24b] M. Lo Vetere,[24a,24b] M. R. Monge,[24a,24b] S. Passaggio,[24a] C. Patrignani,[24a,24b] E. Robutti,[24a] B. Bhuyan,[25] V. Prasad,[25] M. Morii,[26] A. Adametz,[27] U. Uwer,[27] H. M. Lacker,[28] T. Lueck,[28] P. D. Dauncey,[29] U. Mallik,[30] C. Chen,[31] J. Cochran,[31] W. T. Meyer,[31] S. Prell,[31] A. E. Rubin,[31] A. V. Gritsan,[32] N. Arnaud,[33] M. Davier,[33] D. Derkach,[33] G. Grosdidier,[33] F. Le Diberder,[33] A. M. Lutz,[33] B. Malaescu,[33] P. Roudeau,[33] M. H. Schune,[33] A. Stocchi,[33] G. Wormser,[33] D. J. Lange,[34] D. M. Wright,[34] C. A. Chavez,[35] J. P. Coleman,[35] J. R. Fry,[35] E. Gabathuler,[35] D. E. Hutchcroft,[35] D. J. Payne,[35] C. Touramanis,[35] A. J. Bevan,[36] F. Di Lodovico,[36] R. Sacco,[36] M. Sigamani,[36] G. Cowan,[37] D. N. Brown,[38] C. L. Davis,[38] A. G. Denig,[39] M. Fritsch,[39] W. Gradl,[39] K. Griessinger,[39] A. Hafner,[39] E. Prencipe,[39] R. J. Barlow,[40,§] G. Jackson,[40] G. D. Lafferty,[40] E. Behn,[41] R. Cenci,[41] B. Hamilton,[41] A. Jawahery,[41] D. A. Roberts,[41] C. Dallapiccola,[42] R. Cowan,[43] D. Dujmic,[43] G. Sciolla,[43] R. Cheaib,[44] D. Lindemann,[44] P. M. Patel,[44,‖] S. H. Robertson,[44] P. Biassoni,[45a,45b] N. Neri,[45a] F. Palombo,[45a,45b] S. Stracka,[45a,45b] L. Cremaldi,[46] R. Godang,[46,¶] R. Kroeger,[46] P. Sonnek,[46] D. J. Summers,[46] X. Nguyen,[47] M. Simard,[47] P. Taras,[47] G. De Nardo,[48a,48b] D. Monorchio,[48a,48b] G. Onorato,[48a,48b] C. Sciacca,[48a,48b] M. Martinelli,[49] G. Raven,[49] C. P. Jessop,[50] J. M. LoSecco,[50] W. F. Wang,[50] K. Honscheid,[51] R. Kass,[51] J. Brau,[52] R. Frey,[52] N. B. Sinev,[52] D. Strom,[52] E. Torrence,[52] E. Feltresi,[53a,53b] N. Gagliardi,[53a,53b] M. Margoni,[53a,53b] M. Morandin,[53a] M. Posocco,[53a] M. Rotondo,[53a] G. Simi,[53a] F. Simonetto,[53a,53b] R. Stroili,[53a,53b] S. Akar,[54] E. Ben-Haim,[54] M. Bomben,[54] G. R. Bonneaud,[54] H. Briand,[54] G. Calderini,[54] J. Chauveau,[54] O. Hamon,[54] Ph. Leruste,[54] G. Marchiori,[54] J. Ocariz,[54] S. Sitt,[54] M. Biasini,[55a,55b] E. Manoni,[55a,55b] S. Pacetti,[55a,55b] A. Rossi,[55a,55b] C. Angelini,[56a,56b] G. Batignani,[56a,56b] S. Bettarini,[56a,56b] M. Carpinelli,[56a,56b,**] G. Casarosa,[56a,56b] A. Cervelli,[56a,56b] F. Forti,[56a,56b] M. A. Giorgi,[56a,56b] A. Lusiani,[56a,56c] B. Oberhof,[56a,56b] A. Perez,[56a] G. Rizzo,[56a,56b] J. J. Walsh,[56a] D. Lopes Pegna,[57] J. Olsen,[57] A. J. S. Smith,[57] F. Anulli,[58a] R. Faccini,[58a,58b] F. Ferrarotto,[58a] F. Ferroni,[58a,58b] M. Gaspero,[58a,58b] L. Li Gioi,[58a] M. A. Mazzoni,[58a] G. Piredda,[58a] C. Bünger,[59] O. Grünberg,[59] T. Hartmann,[59] T. Leddig,[59] C. Voß,[59] R. Waldi,[59] T. Adye,[60] E. O. Olaiya,[60] F. F. Wilson,[60] S. Emery,[61] G. Hamel de Monchenault,[61] G. Vasseur,[61] Ch. Yèche,[61] D. Aston,[62] R. Bartoldus,[62] J. F. Benitez,[62] C. Cartaro,[62] M. R. Convery,[62] J. Dorfan,[62] G. P. Dubois-Felsmann,[62] W. Dunwoodie,[62] M. Ebert,[62] R. C. Field,[62] M. Franco Sevilla,[62] B. G. Fulsom,[62] A. M. Gabareen,[62] M. T. Graham,[62] P. Grenier,[62] C. Hast,[62] W. R. Innes,[62] M. H. Kelsey,[62] P. Kim,[62] M. L. Kocian,[62] D. W. G. S. Leith,[62] P. Lewis,[62] B. Lindquist,[62] S. Luitz,[62] V. Luth,[62] H. L. Lynch,[62] D. B. MacFarlane,[62] D. R. Muller,[62] H. Neal,[62] S. Nelson,[62] M. Perl,[62] T. Pulliam,[62] B. N. Ratcliff,[62] A. Roodman,[62] A. A. Salnikov,[62] R. H. Schindler,[62] A. Snyder,[62] D. Su,[62] M. K. Sullivan,[62] J. Va'vra,[62] A. P. Wagner,[62] W. J. Wisniewski,[62] M. Wittgen,[62] D. H. Wright,[62] H. W. Wulsin,[62] C. C. Young,[62] V. Ziegler,[62] W. Park,[63] M. V. Purohit,[63] R. M. White,[63] J. R. Wilson,[63] A. Randle-Conde,[64] S. J. Sekula,[64] M. Bellis,[65] P. R. Burchat,[65] T. S. Miyashita,[65] E. M. T. Puccio,[65] M. S. Alam,[66] J. A. Ernst,[66] R. Gorodeisky,[67] N. Guttman,[67] D. R. Peimer,[67] A. Soffer,[67] S. M. Spanier,[68] J. L. Ritchie,[69] A. M. Ruland,[69] R. F. Schwitters,[69] B. C. Wray,[69] J. M. Izen,[70] X. C. Lou,[70] F. Bianchi,[71a,71b] D. Gamba,[71a,71b] S. Zambito,[71a,71b] L. Lanceri,[72a,72b] L. Vitale,[72a,72b] F. Martinez-Vidal,[73] A. Oyanguren,[73] P. Villanueva-Perez,[73] H. Ahmed,[74] J. Albert,[74] Sw. Banerjee,[74] F. U. Bernlochner,[74] H. H. F. Choi,[74] G. J. King,[74] R. Kowalewski,[74] M. J. Lewczuk,[74] I. M. Nugent,[74] J. M. Roney,[74] R. J. Sobie,[74] N. Tasneem,[74] T. J. Gershon,[75] P. F. Harrison,[75] T. E. Latham,[75] H. R. Band,[76] S. Dasu,[76] Y. Pan,[76] R. Prepost,[76] and S. L. Wu[76]

(BABAR Collaboration)

[1]Laboratoire d'Annecy-le-Vieux de Physique des Particules (LAPP), Université de Savoie, CNRS/IN2P3, F-74941 Annecy-Le-Vieux, France
[2]Departament ECM, Facultat de Fisica, Universitat de Barcelona, E-08028 Barcelona, Spain
[3a]INFN Sezione di Bari, I-70126 Bari, Italy
[3b]Dipartimento di Fisica, Università di Bari, I-70126 Bari, Italy
[4]Institute of Physics, University of Bergen, N-5007 Bergen, Norway
[5]Lawrence Berkeley National Laboratory and University of California, Berkeley, California 94720, USA
[6]Ruhr Universität Bochum, Institut für Experimentalphysik 1, D-44780 Bochum, Germany
[7]University of British Columbia, Vancouver, British Columbia, Canada V6T 1Z1
[8]Brunel University, Uxbridge, Middlesex UB8 3PH, United Kingdom
[9]Budker Institute of Nuclear Physics, Novosibirsk 630090, Russia
[10]University of California at Irvine, Irvine, California 92697, USA
[11]University of California at Riverside, Riverside, California 92521, USA
[12]University of California at Santa Barbara, Santa Barbara, California 93106, USA
[13]Institute for Particle Physics, University of California at Santa Cruz, Santa Cruz, California 95064, USA
[14]California Institute of Technology, Pasadena, California 91125, USA
[15]University of Cincinnati, Cincinnati, Ohio 45221, USA
[16]University of Colorado, Boulder, Colorado 80309, USA
[17]Colorado State University, Fort Collins, Colorado 80523, USA
[18]Technische Universität Dortmund, Fakultät Physik, D-44221 Dortmund, Germany
[19]Technische Universität Dresden, Institut für Kern- und Teilchenphysik, D-01062 Dresden, Germany
[20]Laboratoire Leprince-Ringuet, Ecole Polytechnique, CNRS/IN2P3, F-91128 Palaiseau, France
[21]University of Edinburgh, Edinburgh EH9 3JZ, United Kingdom
[22a]INFN Sezione di Ferrara, I-44100 Ferrara, Italy
[22b]Dipartimento di Fisica, Università di Ferrara, I-44100 Ferrara, Italy
[23]INFN Laboratori Nazionali di Frascati, I-00044 Frascati, Italy
[24a]INFN Sezione di Genova, I-16146 Genova, Italy
[24b]Dipartimento di Fisica, Università di Genova, I-16146 Genova, Italy
[25]Indian Institute of Technology Guwahati, Guwahati, Assam, 781 039, India
[26]Harvard University, Cambridge, Massachusetts 02138, USA
[27]Universität Heidelberg, Physikalisches Institut, Philosophenweg 12, D-69120 Heidelberg, Germany
[28]Humboldt-Universität zu Berlin, Institut für Physik, Newtonstr. 15, D-12489 Berlin, Germany
[29]Imperial College London, London, SW7 2AZ, United Kingdom
[30]University of Iowa, Iowa City, Iowa 52242, USA
[31]Iowa State University, Ames, Iowa 50011-3160, USA
[32]Johns Hopkins University, Baltimore, Maryland 21218, USA
[33]Laboratoire de l'Accélérateur Linéaire, IN2P3/CNRS et Université Paris-Sud 11, Centre Scientifique d'Orsay, B. P. 34, F-91898 Orsay Cedex, France
[34]Lawrence Livermore National Laboratory, Livermore, California 94550, USA
[35]University of Liverpool, Liverpool L69 7ZE, United Kingdom
[36]Queen Mary, University of London, London, E1 4NS, United Kingdom
[37]University of London, Royal Holloway and Bedford New College, Egham, Surrey TW20 0EX, United Kingdom
[38]University of Louisville, Louisville, Kentucky 40292, USA
[39]Johannes Gutenberg-Universität Mainz, Institut für Kernphysik, D-55099 Mainz, Germany
[40]University of Manchester, Manchester M13 9PL, United Kingdom
[41]University of Maryland, College Park, Maryland 20742, USA
[42]University of Massachusetts, Amherst, Massachusetts 01003, USA
[43]Massachusetts Institute of Technology, Laboratory for Nuclear Science, Cambridge, Massachusetts 02139, USA
[44]McGill University, Montréal, Québec, Canada H3A 2T8
[45a]INFN Sezione di Milano, I-20133 Milano, Italy
[45b]Dipartimento di Fisica, Università di Milano, I-20133 Milano, Italy
[46]University of Mississippi, University, Mississippi 38677, USA
[47]Université de Montréal, Physique des Particules, Montréal, Québec, Canada H3C 3J7
[48a]INFN Sezione di Napoli, I-80126 Napoli, Italy
[48b]Dipartimento di Scienze Fisiche, Università di Napoli Federico II, I-80126 Napoli, Italy
[49]NIKHEF, National Institute for Nuclear Physics and High Energy Physics, NL-1009 DB Amsterdam, The Netherlands
[50]University of Notre Dame, Notre Dame, Indiana 46556, USA
[51]Ohio State University, Columbus, Ohio 43210, USA

[52]*University of Oregon, Eugene, Oregon 97403, USA*
[53a]*INFN Sezione di Padova, I-35131 Padova, Italy*
[53b]*Dipartimento di Fisica, Università di Padova, I-35131 Padova, Italy*
[54]*Laboratoire de Physique Nucléaire et de Hautes Energies, IN2P3/CNRS, Université Pierre et Marie Curie-Paris6, Université Denis Diderot-Paris7, F-75252 Paris, France*
[55a]*INFN Sezione di Perugia, I-06100 Perugia, Italy*
[55b]*Dipartimento di Fisica, Università di Perugia, I-06100 Perugia, Italy*
[56a]*INFN Sezione di Pisa, I-56127 Pisa, Italy*
[56b]*Dipartimento di Fisica, Università di Pisa, I-56127 Pisa, Italy*
[56c]*Scuola Normale Superiore di Pisa, I-56127 Pisa, Italy*
[57]*Princeton University, Princeton, New Jersey 08544, USA*
[58a]*INFN Sezione di Roma, I-00185 Roma, Italy*
[58b]*Dipartimento di Fisica, Università di Roma La Sapienza, I-00185 Roma, Italy*
[59]*Universität Rostock, D-18051 Rostock, Germany*
[60]*Rutherford Appleton Laboratory, Chilton, Didcot, Oxon OX11 0QX, United Kingdom*
[61]*CEA, Irfu, SPP, Centre de Saclay, F-91191 Gif-sur-Yvette, France*
[62]*SLAC National Accelerator Laboratory, Stanford, California 94309, USA*
[63]*University of South Carolina, Columbia, South Carolina 29208, USA*
[64]*Southern Methodist University, Dallas, Texas 75275, USA*
[65]*Stanford University, Stanford, California 94305-4060, USA*
[66]*State University of New York, Albany, New York 12222, USA*
[67]*School of Physics and Astronomy, Tel Aviv University, Tel Aviv, 69978, Israel*
[68]*University of Tennessee, Knoxville, Tennessee 37996, USA*
[69]*University of Texas at Austin, Austin, Texas 78712, USA*
[70]*University of Texas at Dallas, Richardson, Texas 75083, USA*
[71a]*INFN Sezione di Torino, I-10125 Torino, Italy*
[71b]*Dipartimento di Fisica Sperimentale, Università di Torino, I-10125 Torino, Italy*
[72a]*INFN Sezione di Trieste, I-34127 Trieste, Italy*
[72b]*Dipartimento di Fisica, Università di Trieste, I-34127 Trieste, Italy*
[73]*IFIC, Universitat de Valencia-CSIC, E-46071 Valencia, Spain*
[74]*University of Victoria, Victoria, British Columbia, Canada V8W 3P6*
[75]*Department of Physics, University of Warwick, Coventry CV4 7AL, United Kingdom*
[76]*University of Wisconsin, Madison, Wisconsin 53706, USA*
(Received 7 January 2013; published 22 March 2013)

We report the determination of the Cabibbo-Kobayashi-Maskawa *CP*-violating angle γ through the combination of various measurements involving $B^{\pm} \to DK^{\pm}$, $B^{\pm} \to D^{*}K^{\pm}$, and $B^{\pm} \to DK^{*\pm}$ decays performed by the *BABAR* experiment at the PEP-II $e^{+}e^{-}$ collider at SLAC National Accelerator Laboratory. Using up to 474 million $B\bar{B}$ pairs, we obtain $\gamma = (69^{+17}_{-16})^{\circ}$ modulo 180°. The total uncertainty is dominated by the statistical component, with the experimental and amplitude-model systematic uncertainties amounting to $\pm 4^{\circ}$. The corresponding two-standard-deviation region is $41^{\circ} < \gamma < 102^{\circ}$. This result is inconsistent with $\gamma = 0$ with a significance of 5.9 standard deviations.

DOI: 10.1103/PhysRevD.87.052015 PACS numbers: 13.25.Hw, 11.30.Er, 12.15.Hh, 14.40.Nd

I. INTRODUCTION AND OVERVIEW

In the Standard Model (SM), the mechanism of *CP* violation in weak interactions arises from the joint effect of three mixing angles and the single irreducible phase in the three-family Cabibbo-Kobayashi-Maskawa (CKM) quark-mixing matrix [1]. The unitarity of the CKM matrix V implies a set of relations among its elements, V_{ij}, with $i = u, c, t$ and $j = d, s, b$. In particular, $V_{ud}V^{*}_{ub} + V_{cd}V^{*}_{cb} + V_{td}V^{*}_{tb} = 0$, which can be depicted in the complex plane as a unitarity triangle whose sides and angles are related to the magnitudes and phases of the six elements of the first and third columns of the matrix, V_{id} and V_{ib}. The parameter γ, defined as $\arg[-V_{ud}V^{*}_{ub}/V_{cd}V^{*}_{cb}]$, is one of the three angles of this triangle. From measurements of the sides and angles of the unitarity triangle from many decay processes, it is possible to overconstrain our knowledge of the CKM mechanism, probing dynamics beyond the

[*]Now at the University of Tabuk, Tabuk 71491, Saudi Arabia.
[†]Present address: the European Organization for Nuclear Research (CERN), Geneva, Switzerland.
[‡]Also at Università di Perugia, Dipartimento di Fisica, Perugia, Italy.
[§]Present address: the University of Huddersfield, Huddersfield HD1 3DH, United Kingdom.
[∥]Deceased.
[¶]Present address: the University of South Alabama, Mobile, Alabama 36688, USA.
[**]Also at Università di Sassari, Sassari, Italy.

SM [2]. In this context, the angle γ is particularly relevant since it is the only CP-violating parameter that can be cleanly determined using tree-level B meson decays [3]. In spite of a decade of successful operation and experimental efforts by the B factory experiments, *BABAR* and Belle, γ is poorly known due to its large statistical uncertainty. Its precise determination is an important goal of present and future flavor-physics experiments.

Several methods have been pursued to extract γ [4–9]. Those using charged B meson decays into $D^{(*)}K^{\pm}$ and $DK^{*\pm}$ final states, denoted generically as $D^{(*)}K^{(*)\pm}$, yield low theoretical uncertainties since the decays involved do not receive contributions from penguin diagrams (see Fig. 1). This is a very important distinction from most other measurements of the angles. Here, the symbol $D^{(*)}$ indicates either a D^0 (D^{*0}) or a $\bar{D}^0$ ($\bar{D}^{*0}$) meson, and $K^{*\pm}$ refers to $K^*(892)^{\pm}$ states. The methods to measure γ based on $B^{\pm} \to D^{(*)}K^{(*)\pm}$ decays rely on the interference between the CKM- and color-favored $b \to c\bar{u}s$ and the suppressed $b \to u\bar{c}s$ amplitudes, which arises when the D^0 from a $B^- \to D^0K^-$ decay [10] (and similarly for the other related B decays) is reconstructed in a final state which can be produced also in the decay of a $\bar{D}^0$ originating from $B^- \to \bar{D}^0K^-$ (see Fig. 1). The interference between the $b \to c\bar{u}s$ and $b \to u\bar{c}s$ tree amplitudes results in observables that depend on their relative weak phase γ, on the magnitude ratio $r_B \equiv |\mathcal{A}(b \to u\bar{c}s)/\mathcal{A}(b \to c\bar{u}s)|$, and on the relative strong phase δ_B between the two amplitudes. In the case of a nonzero weak phase γ and a nonzero strong phase δ_B, the B^- and B^+ decay rates are different, which is a manifestation of direct CP violation. The hadronic parameters r_B and δ_B are not precisely known from theory, and may have different values for $DK^{\pm}$, $D^*K^{\pm}$, and $DK^{*\pm}$ final states. They can be measured directly from data by simultaneously reconstructing several D-decay final states.

The three main approaches employed by the B factory experiments are:

(i) the Dalitz plot or Giri-Grossman-Soffer-Zupan (GGSZ) method, based on three-body, self-conjugate final states, such as $K_S^0\pi^+\pi^-$ [7];

(ii) the Gronau-London-Wyler (GLW) method, based on decays to CP-eigenstate final states, such as K^+K^- and $K_S^0\pi^0$ [8];

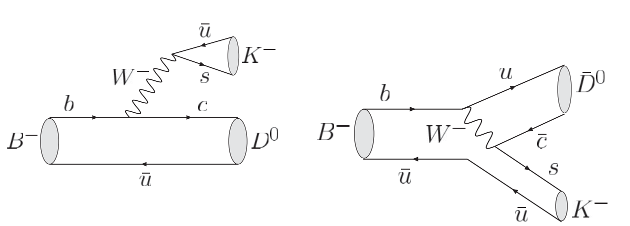

FIG. 1. Dominant Feynman diagrams for the decays $B^- \to D^0K^-$ (left) and $B^- \to \bar{D}^0K^-$ (right). The left diagram proceeds via $b \to c\bar{u}s$ transition, while the right diagram proceeds via $b \to u\bar{c}s$ transition and is both CKM- and color-suppressed.

(iii) the Atwood-Dunietz-Soni (ADS) method, based on D decays to doubly-Cabibbo-suppressed final states, such as $D^0 \to K^+\pi^-$ [9].

To date, the GGSZ method has provided the highest statistical power in measuring γ. The other two methods provide additional information that can further constrain the hadronic parameters and thus allow for a more robust determination of γ. The primary issue with all these methods is the small product branching fraction of the decays involved, which range from 5×10^{-6} to 5×10^{-9}, and the small size of the interference, proportional to $r_B \approx c_F|V_{cs}V_{ub}^*|/|V_{us}V_{cb}^*| \approx 0.1$, where $c_F \approx 0.2$ is a color suppression factor [11–13]. Therefore a precise determination of γ requires a very large data sample and the combination of all available methods involving different D decay modes.

Recently, Belle [14] and LHCb [15] have presented the preliminary results of the combination of their measurements related to γ, yielding γ to be $(68^{+15}_{-14})°$ and $(71^{+17}_{-16})°$, respectively. Attempts to combine the results by *BABAR*, Belle, CDF, and LHCb have been performed by the CKMfitter and UTfit groups [2]. Their most recent results are $(66 \pm 12)°$ and $(72 \pm 9)°$, respectively.

The *BABAR* experiment [16] at the PEP-II asymmetric-energy e^+e^- collider at SLAC has analyzed charged B decays into $DK^{\pm}$, $D^*K^{\pm}$, and $DK^{*\pm}$ final states using the GGSZ [17–19], GLW [20–22], and ADS [22–24] methods, providing a variety of measurements and constraints on γ. The results are based on a data set collected at a center-of-mass energy equal to the mass of the $\Upsilon(4S)$ resonance, and about 10% of data collected 40 MeV below. We present herein the combination of published *BABAR* measurements using detailed information on correlations between parameters that we have not previously published. This combination represents the most complete study of the data sample collected by *BABAR* and benefits from the possibility to access and reanalyze the data sample (see Sec. II for details).

Other analyses related to γ [25–27] or $2\beta + \gamma$ [28,29] have not been included, because the errors on the experimental measurements are too large.

II. INPUT MEASUREMENTS

In the GGSZ approach, where D mesons are reconstructed into the $K_S^0\pi^+\pi^-$ and $K_S^0K^+K^-$ final states [17–19], the signal rates for $B^{\pm} \to D^{(*)}K^{\pm}$ and $B^{\pm} \to DK^{*\pm}$ decays are analyzed as a function of the position in the Dalitz plot of squared invariant masses $m_-^2 \equiv m^2(K_S^0h^-)$, $m_+^2 \equiv m^2(K_S^0h^+)$, where h is either a charged pion or kaon ($h = \pi$, K). We assume no CP violation in the neutral D and K meson systems and neglect small $D^0 - \bar{D}^0$ mixing effects [30,31], leading to $\bar{\mathcal{A}}(m_-^2, m_+^2) = \mathcal{A}(m_+^2, m_-^2)$, where $\bar{\mathcal{A}}$ ($\mathcal{A}$) is the $\bar{D}^0$ (D^0) decay amplitude. In this case, the signal decay rates can be written as [32]

$$\Gamma_{\pm}^{(*)}(m_{-}^{2}, m_{+}^{2}) \propto |\mathcal{A}_{\pm}|^{2} + r_{B^{\pm}}^{(*)\,2}|\mathcal{A}_{\mp}|^{2} + 2\lambda \mathrm{Re}[\mathsf{z}_{\pm}^{(*)}\mathcal{A}_{\pm}^{\dagger}\mathcal{A}_{\mp}],$$
$$\Gamma_{\pm}^{s}(m_{-}^{2}, m_{+}^{2}) \propto |\mathcal{A}_{\pm}|^{2} + r_{s\pm}^{2}|\mathcal{A}_{\mp}|^{2} + 2\mathrm{Re}[\mathsf{z}_{s\pm}\mathcal{A}_{\pm}^{\dagger}\mathcal{A}_{\mp}], \quad (1)$$

with $\mathcal{A}_{\pm} \equiv \mathcal{A}(m_{\pm}^{2}, m_{\mp}^{2})$ and $\mathcal{A}_{\pm}^{\dagger}$ is the complex conjugate of $\mathcal{A}_{\pm}$. The symbol λ for $B^{\pm} \to D^{*}K^{\pm}$ accounts for the different *CP* parity of the D^{*} when it is reconstructed into $D\pi^{0}$ ($\lambda = +1$) and $D\gamma$ ($\lambda = -1$) final states, as a consequence of the opposite *CP* eigenvalue of the π^{0} and the photon [33]. Here, $r_{B^{\pm}}^{(*)}$ and $r_{s\pm}$ are the magnitude ratios between the $b \to u\bar{c}s$ and $b \to c\bar{u}s$ amplitudes for $B^{\pm} \to D^{(*)}K^{\pm}$ and $B^{\pm} \to DK^{*\pm}$ decays, respectively, and $\delta_{B}^{(*)}$, δ_{s} are their relative strong phases. The analysis extracts the *CP*-violating observables [19]

$$\mathsf{z}_{\pm}^{(*)} \equiv x_{\pm}^{(*)} + iy_{\pm}^{(*)}, \qquad \mathsf{z}_{s\pm} \equiv x_{s\pm} + iy_{s\pm}, \quad (2)$$

defined as the suppressed-to-favored complex amplitude ratios $\mathsf{z}_{\pm}^{(*)} = r_{B^{\pm}}^{(*)}e^{i(\delta_{B}^{(*)} \pm \gamma)}$ and $\mathsf{z}_{s\pm} = \kappa r_{s\pm}e^{i(\delta_{s} \pm \gamma)}$, for $B^{\pm} \to D^{(*)}K^{\pm}$ and $B^{\pm} \to DK^{*\pm}$ decays, respectively. The hadronic parameter κ is defined as

$$\kappa e^{i\delta_{s}} \equiv \frac{\int A_{c}(p)A_{u}(p)e^{i\delta(p)}\mathrm{d}p}{\sqrt{\int A_{c}^{2}(p)\mathrm{d}p \int A_{u}^{2}(p)\mathrm{d}p}}, \quad (3)$$

where $A_{c}(p)$ and $A_{u}(p)$ are the magnitudes of the $b \to c\bar{u}s$ and $b \to u\bar{c}s$ amplitudes as a function of the $B^{\pm} \to DK_{S}^{0}\pi^{\pm}$ phase-space position p, and $\delta(p)$ is their relative strong phase. This coherence factor, with $0 < \kappa < 1$ in the most general case and $\kappa = 1$ for two-body B decays, accounts for the interference between $B^{\pm} \to DK^{*\pm}$ and other $B^{\pm} \to DK_{S}^{0}\pi^{\pm}$ decays, as a consequence of the $K^{*\pm}$ natural width [12]. In our analysis, κ has been fixed to 0.9 and a systematic uncertainty has been assigned, varying its value by ± 0.1, as estimated using a Monte Carlo simulation based on the Dalitz plot model of $B^{\pm} \to DK_{S}^{0}\pi^{\pm}$ decays [18]. Thus the parameter δ_{s} is an effective strong-phase difference averaged over the phase space.

Table I summarizes our experimental results for the *CP*-violating parameters $\mathsf{z}_{\pm}^{(*)}$ and $\mathsf{z}_{s\pm}$. Complete 12×12 covariance matrices for statistical, experimental systematic, and amplitude-model uncertainties are reported in Ref. [17]. The $\mathsf{z}_{\pm}^{(*)}$ and $\mathsf{z}_{s\pm}$ observables are unbiased and have Gaussian behavior with small correlations, even for low values of $r_{B}^{(*)}$, κr_{s} and relatively low-statistics samples. Furthermore, their uncertainties have a minimal dependence on their central values and are free of physical bounds [19]. These good statistical properties allow for easier combination of several measurements into a single result. For example, the rather complex experimental GGSZ likelihood function can be parametrized by a 12-dimensional (correlated) Gaussian probability density function (P.D.F.), defined in the space of the $\mathsf{z}_{\pm}^{(*)}$ and $\mathsf{z}_{s\pm}$ measurements from Table I. After this combination has been performed, the values of γ and of the hadronic parameters $r_{B}^{(*)}$, κr_{s}, $\delta_{B}^{(*)}$, and δ_{s} can be obtained.

TABLE I. *CP*-violating complex parameters $\mathsf{z}_{\pm}^{(*)} \equiv x_{\pm}^{(*)} + iy_{\pm}^{(*)}$ and $\mathsf{z}_{s\pm} \equiv x_{s\pm} + iy_{s\pm}$, measured using the GGSZ technique [17]. The first uncertainty is statistical, the second is the experimental systematic uncertainty and the third is the systematic uncertainty associated with the D^{0} decay amplitude models. The sample analyzed contains 468 million $B\bar{B}$ pairs.

	Real part (%)	Imaginary part (%)
z_{-}	$6.0 \pm 3.9 \pm 0.7 \pm 0.6$	$6.2 \pm 4.5 \pm 0.4 \pm 0.6$
z_{+}	$-10.3 \pm 3.7 \pm 0.6 \pm 0.7$	$-2.1 \pm 4.8 \pm 0.4 \pm 0.9$
z_{-}^{*}	$-10.4 \pm 5.1 \pm 1.9 \pm 0.2$	$-5.2 \pm 6.3 \pm 0.9 \pm 0.7$
z_{+}^{*}	$14.7 \pm 5.3 \pm 1.7 \pm 0.3$	$-3.2 \pm 7.7 \pm 0.8 \pm 0.6$
z_{s-}	$7.5 \pm 9.6 \pm 2.9 \pm 0.7$	$12.7 \pm 9.5 \pm 2.7 \pm 0.6$
z_{s+}	$-15.1 \pm 8.3 \pm 2.9 \pm 0.6$	$4.5 \pm 10.6 \pm 3.6 \pm 0.8$

The D decay amplitudes $\mathcal{A}_{\pm}$ have been determined from Dalitz plot analyses of tagged D^{0} mesons from $D^{*+} \to D^{0}\pi^{+}$ decays produced in $e^{+}e^{-} \to c\bar{c}$ events [18,34], assuming an empirical model to describe the variation of the amplitude phase as a function of the Dalitz plot variables. A model-independent, binned approach also exists [7,35], which optimally extracts information on γ for higher-statistics samples than the ones available. This type of analysis has been performed as a proof of principle by the Belle collaboration [36], giving consistent results to the model-dependent approach [37]. The LHCb collaboration has also released results of a model-independent GGSZ analysis [38].

In order to determine γ with the GLW method, the analyses measure the direct *CP*-violating partial decay rate asymmetries

$$A_{CP\pm}^{(*)} \equiv \frac{\Gamma(B^{-} \to D_{CP\pm}^{(*)}K^{-}) - \Gamma(B^{+} \to D_{CP\pm}^{(*)}K^{+})}{\Gamma(B^{-} \to D_{CP\pm}^{(*)}K^{-}) + \Gamma(B^{+} \to D_{CP\pm}^{(*)}K^{+})}, \quad (4)$$

and the ratios of charge-averaged partial rates using D decays to *CP* and flavor eigenstates,

$$R_{CP\pm}^{(*)} \equiv 2\frac{\Gamma(B^{-} \to D_{CP\pm}^{(*)}K^{-}) + \Gamma(B^{+} \to D_{CP\pm}^{(*)}K^{+})}{\Gamma(B^{-} \to D^{(*)0}K^{-}) + \Gamma(B^{+} \to \bar{D}^{(*)0}K^{+})}, \quad (5)$$

where $D_{CP\pm}^{(*)}$ refers to the *CP* eigenstates of the $D^{(*)}$ meson system. We select D mesons in the *CP*-even eigenstates $\pi^{-}\pi^{+}$ and $K^{-}K^{+}$ (D_{CP+}), in the *CP*-odd eigenstates $K_{S}^{0}\pi^{0}$, $K_{S}^{0}\phi$, and $K_{S}^{0}\omega$ (D_{CP-}), and in the non-*CP* eigenstate $K^{-}\pi^{+}$ (D^{0} from $B^{-} \to D^{0}h^{-}$) or $K^{+}\pi^{-}$ ($\bar{D}^{0}$ from $B^{+} \to \bar{D}^{0}h^{+}$). We recontruct D^{*} mesons in the states $D\pi^{0}$ and $D\gamma$. The observables $A_{CP\pm}^{s}$ and $R_{CP\pm}^{s}$ for $B^{\pm} \to DK^{*\pm}$ decays are defined similarly.

For later convenience, the GLW observables can be related to $z_{\pm}^{(*)}$ and $z_{s\pm}$ (neglecting mixing and CP violation in neutral D decays) as

$$A_{CP\pm}^{(*)} = \pm \frac{x_{-}^{(*)} - x_{+}^{(*)}}{1 + |z^{(*)}|^2 \pm (x_{-}^{(*)} + x_{+}^{(*)})} \tag{6}$$

and

$$R_{CP\pm}^{(*)} = 1 + |z^{(*)}|^2 \pm (x_{-}^{(*)} + x_{+}^{(*)}), \tag{7}$$

where $|z^{(*)}|^2$ is the average value of $|z_{+}^{(*)}|^2$ and $|z_{-}^{(*)}|^2$. For $B^\pm \to DK^{*\pm}$ decays, similar relations to Eqs. (6) and (7) hold, with $\kappa = 1$, since the effects of the non-K^* $B \to DK\pi$ events and the width of the K^* are incorporated into the systematic uncertainties of the $A_{CP\pm}^{s}$ and $R_{CP\pm}^{s}$ measurements [22].

Table II summarizes the results obtained for the GLW observables. In order to avoid overlaps with the samples selected in the Dalitz plot analysis, the results for $B^\pm \to D_{CP-}K^\pm$ decays are corrected by removing the contribution from $D_{CP-} \to K_S^0\phi$, $\phi \to K^+K^-$ candidates [20]. For the decays $B^\pm \to D^*_{CP-}[D_{CP-}\pi^0]K^\pm$, $B^\pm \to D^*_{CP+}[D_{CP-}\gamma]K^\pm$, and $B^\pm \to D_{CP-}K^{*\pm}$, such information is not available. In this case, the overlap is accounted for by increasing the uncertainties quoted in Refs. [21,22] by 10% while keeping the central values unchanged. The 10% increase in the experimental uncertainties is approximately the change observed in $B^\pm \to D_{CP-}K^\pm$ decays when excluding or including $D \to K_S^0\phi$ in the measurement. The impact on the combination has been found to be negligible.

As in the case of the GGSZ observables, $A_{CP\pm}^{(*)}$, $A_{CP\pm}^{s}$, $R_{CP\pm}^{(*)}$, and $R_{CP\pm}^{s}$ have Gaussian uncertainties near the best solution, with small statistical and systematic correlations, as given in Ref. [20] for $B^\pm \to D_{CP-}K^\pm$ decays. The GLW method has also been exploited by the Belle [39], CDF [40], and LHCb collaborations [41], with consistent results.

TABLE II. GLW observables measured for the $B^\pm \to DK^\pm$ (based on 467 million $B\bar{B}$ pairs) [20], $B^\pm \to D^*K^\pm$ (383 million $B\bar{B}$ pairs) [21], and $B^\pm \to DK^{*\pm}$ (379 million $B\bar{B}$ pairs) [22] decays, corrected by removing the contribution from $D_{CP-} \to K_S^0\phi$, $\phi \to K^+K^-$ candidates. The first uncertainty is statistical, the second is systematic.

	CP-even	CP-odd
$R_{CP\pm}$	$1.18 \pm 0.09 \pm 0.05$	$1.03 \pm 0.09 \pm 0.04$
$A_{CP\pm}$	$0.25 \pm 0.06 \pm 0.02$	$-0.08 \pm 0.07 \pm 0.02$
$R^*_{CP\pm}$	$1.31 \pm 0.13 \pm 0.04$	$1.10 \pm 0.13 \pm 0.04$
$A^*_{CP\pm}$	$-0.11 \pm 0.09 \pm 0.01$	$0.06 \pm 0.11 \pm 0.02$
$R^s_{CP\pm}$	$2.17 \pm 0.35 \pm 0.09$	$1.03 \pm 0.30 \pm 0.14$
$A^s_{CP\pm}$	$0.09 \pm 0.13 \pm 0.06$	$-0.23 \pm 0.23 \pm 0.08$

In the ADS method, the D^0 meson from the favored $b \to c\bar{u}s$ amplitude is reconstructed in the doubly-Cabibbo-suppressed decay $K^+\pi^-$, while the $\bar{D}^0$ from the $b \to u\bar{c}s$ suppressed amplitude is reconstructed in the favored decay $K^+\pi^-$ [22,23]. The product branching fractions for these final states, which we denote as $B^- \to [K^+\pi^-]_D K^-$, $B^- \to [K^+\pi^-]^*_D K^-$, $B^- \to [K^+\pi^-]_D K^{*-}$, and their CP conjugates, are small ($\sim 10^{-7}$). However, the two interfering amplitudes are of the same order of magnitude, allowing for possible large CP asymmetries. We measure charge-specific ratios for B^+ and B^- decay rates to the ADS final states, which are defined as

$$R_{\pm}^{(*)} \equiv \frac{\Gamma(B^\pm \to [K^\mp\pi^\pm]_D^{(*)}K^\pm)}{\Gamma(B^\pm \to [K^\pm\pi^\mp]_D^{(*)}K^\pm)}, \tag{8}$$

and similarly for $R^s_{\pm}$, where the favored decays $B^- \to [K^-\pi^+]_D K^-$, $B^- \to [K^-\pi^+]^*_D K^-$, and $B^- \to [K^-\pi^+]_D K^{*-}$ serve as normalization so that many systematic uncertainties cancel. The rates in Eq. (8) depend on γ and the B-decay hadronic parameters. They are related to $z_{\pm}^{(*)}$ and $z_{s\pm}$ through

$$R_{\pm}^{(*)} = r_{B^\pm}^{(*)\,2} + r_D^2 + 2\lambda r_D\Big[x_{\pm}^{(*)}\cos\delta_D - y_{\pm}^{(*)}\sin\delta_D\Big], \tag{9}$$

where $r_D = |\mathcal{A}(D^0 \to K^+\pi^-)/\mathcal{A}(D^0 \to K^-\pi^+)|$ and δ_D are the ratio between magnitudes of the suppressed and favored D-decay amplitudes and their relative strong phase, respectively. As in Eq. (1), the symbol λ for $B^\pm \to D^*K^\pm$ decays accounts for the different CP parity of $D^* \to D\pi^0$ and $D^* \to D\gamma$. The values of r_D and δ_D are taken as external constraints in our analysis. As for the GLW method, the effects of other $B^\pm \to DK_S^0\pi^\pm$ events, not going through $K^{*\pm}$, and the $K^{*\pm}$ width, are incorporated in the systematic uncertainties on $R^s_{\pm}$. Thus similar relations hold for these observables with $\kappa = 1$.

The choice of the observables $R_\pm$ (and similarly for $R^*_\pm$ and $R^s_\pm$) rather than the original ADS observables $R_{\rm ADS} \equiv (R_+ + R_-)/2$ and $A_{\rm ADS} \equiv (R_- - R_+)/2R_{\rm ADS}$ [9] is motivated by the fact that the set of variables $(R_{\rm ADS}, A_{\rm ADS})$ is not well-behaved since the uncertainty on $A_{\rm ADS}$ depends on the central value of $R_{\rm ADS}$, while R_+ and R_- are statistically independent observables. Although systematic uncertainties are largely correlated, the measurements of R_+ and R_- are effectively uncorrelated since the total uncertainties are dominated by the statistical component.

We have also reconstructed $B^\pm \to [K^\mp\pi^\pm\pi^0]_D K^\pm$ decays [24] from which the observables $R_{\pm}^{K\pi\pi^0}$ have been measured, which are related to the GGSZ observables as

$$R_{\pm}^{K\pi\pi^0} = r_{B^\pm}^2 + r_{K\pi\pi^0}^2 + 2\kappa_{K\pi\pi^0} r_{K\pi\pi^0}[x_\pm\cos\delta_{K\pi\pi^0} - y_\pm\sin\delta_{K\pi\pi^0}], \tag{10}$$

where $\kappa_{K\pi\pi^0}$ is a D decay coherence factor similar to that defined in Eq. (3) for the $B^\pm \to DK_S^0\pi^\pm$ decay, and where $r_{K\pi\pi^0}$ and $\delta_{K\pi\pi^0}$ are hadronic parameters for $D^0 \to K^\pm\pi^\mp\pi^0$ decays analogous to r_D and δ_D.

TABLE III. ADS observables included into the combination for $B^{\pm} \to DK^{\pm}$ with $D \to K\pi$ (based on 467 million $B\bar{B}$ pairs) and $D \to K\pi\pi^0$ (based on 474 million $B\bar{B}$ pairs), $B^{\pm} \to D^* K^{\pm}$ (467 million $B\bar{B}$ pairs), and $B^{\pm} \to DK^{*\pm}$ (379 million $B\bar{B}$ pairs) decays [22–24]. The first uncertainty is statistical, the second is systematic.

	B^+	B^-
$R_{\pm}$	$0.022 \pm 0.009 \pm 0.003$	$0.002 \pm 0.006 \pm 0.002$
$R^*_{\pm}$ $[D\pi^0]$	$0.005 \pm 0.008 \pm 0.003$	$0.037 \pm 0.018 \pm 0.009$
$R^*_{\pm}$ $[D\gamma]$	$0.009 \pm 0.016 \pm 0.007$	$0.019 \pm 0.023 \pm 0.012$
$R^s_{\pm}$	$0.076 \pm 0.042 \pm 0.011$	$0.054 \pm 0.049 \pm 0.011$
$R^{K\pi\pi^0}_{\pm}$	$0.005^{+0.012+0.001}_{-0.010-0.004}$	$0.012^{+0.012+0.002}_{-0.010-0.004}$

Table III summarizes the measurements of the ADS charge-specific ratios for the different final states. Contrary to the case of the GGSZ and GLW observables, $R^{(*)}_{\pm}$, $R^s_{\pm}$, and $R^{K\pi\pi^0}_{\pm}$ do not have Gaussian behavior. The experimental likelihood function for each of the four decay modes, shown in Fig. 2 for $B^{\pm} \to DK^{\pm}$ and $B^{\pm} \to D^*K^{\pm}$ decays, is well described around the best solution by an analytical P.D.F. composed of the sum of two asymmetric Gaussian functions. For the $B^{\pm} \to DK^{*\pm}$ channel, we use instead a simple Gaussian approximation since in this case the experimental likelihood scans are not available. The effect of this approximation has been verified to be negligible, given the small statistical weight of this sample in the combination. Measurements using the ADS technique have also been performed by the Belle [42,43], CDF [44], and LHCb collaborations [41], with consistent results.

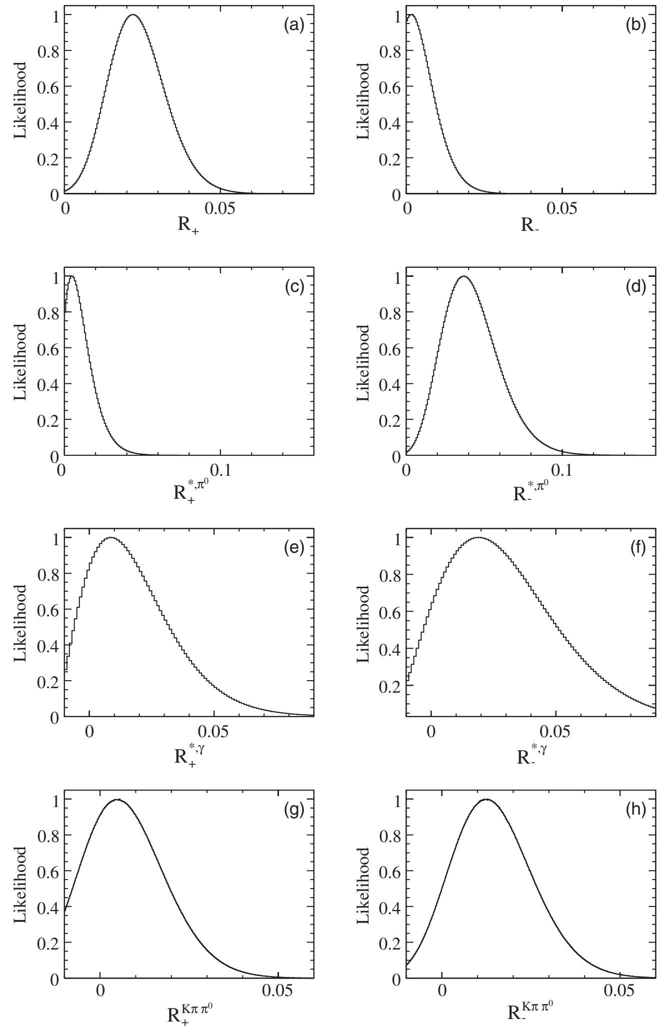

FIG. 2. Experimental likelihoods as functions of the ADS charge-specific ratios $R_{\pm}$ (a,b), $R^*_{\pm}$ $[D\pi^0]$ (c,d), $R^*_{\pm}$ $[D\gamma]$ (e,f), and $R^{K\pi\pi^0}_{\pm}$ (g,h), from Refs. [23,24], including systematic uncertainties. The P.D.F.s are normalized so that their maximum values are equal to 1. These distributions are well parametrized by sums of two asymmetric Gaussian functions with mean values as given in Table III.

III. OTHER MEASUREMENTS

Similar analyses related to γ measurement have been carried out using the decay $B^- \to DK^-$ with the $D \to \pi^+\pi^-\pi^0$ final state [25], and the neutral B decay $\bar{B}^0 \to D\bar{K}^*(892)^0$, $\bar{K}^*(892)^0 \to K^-\pi^+$, with $D \to K^0_S\pi^+\pi^-$ [26] and $D \to K^{\pm}\pi^{\mp}$, $K^{\pm}\pi^{\mp}\pi^0$, $K^{\pm}\pi^{\mp}\pi^{\pm}\pi^{\mp}$ [27]. For neutral B decays, r_B is naively expected to be larger (≈ 0.3) because both interfering amplitudes are color suppressed and thus $c_F \approx 1$. However, the overall rate of events is smaller than for $B^- \to DK^{*-}$ decays. The flavor of the neutral B meson is tagged by the charge of the kaon produced in the $\bar{K}^{*0}$ decay, $\bar{K}^*(892)^0 \to K^-\pi^+$ or $K^*(892)^0 \to K^+\pi^-$.

Experimental analyses of the time-dependent decay rates of $B \to D^{(*)\mp}\pi^{\pm}$ and $B \to D^{\mp}\rho(770)^{\pm}$ decays have also been used to constrain γ [28,29]. In these decays, the interference occurs between the favored $b \to c\bar{u}d$ and the suppressed $b \to u\bar{c}d$ tree amplitudes with and without $B^0 - \bar{B}^0$ mixing, resulting in a total weak-phase difference $2\beta + \gamma$ [45], where β is the angle of the unitarity triangle defined as $\arg[-V_{cd}V^*_{cb}/V_{td}V^*_{tb}]$. The magnitude ratios between the suppressed and favored amplitudes $r_{D^{(*)}\pi}$ and $r_{D\rho}$ are expected to be $\approx 2\%$, and have to be estimated either by analyzing suppressed charged B decays (e.g., $B^+ \to D^+\pi^0$) with an isospin assumption or from self-tagging neutral B decays to charmed-strange mesons (e.g., $B^0 \to D^+_s\pi^-$) assuming SU(3) flavor symmetry and neglecting contributions from W-exchange diagrams [45]. Performing a time-dependent Dalitz plot analysis of $B \to D^{\mp}K^0\pi^{\pm}$ decays [46] could in principle avoid the problem of the smallness of r. In these decays the two interfering amplitudes are color suppressed, and it is expected to be ≈ 0.3, but the overall rate of events is too small with the current data sample.

In both cases, the errors on the experimental measurements are too large for a meaningful determination of γ, and have not been included in the combined determination of γ reported in this paper. However, these decay channels might provide important information in future experiments.

IV. COMBINATION PROCEDURE

We combine all the GGSZ, GLW, and ADS observables (34 in total) to extract γ in two different stages. First, we extract the best-fit values for the CP-violating quantities $\bar{\mathbf{z}}_{\pm}^{(*)}$ and $\bar{\mathbf{z}}_{s\pm}$, whose definitions correspond to those for the quantities $\mathbf{z}_{\pm}^{(*)}$ and $\mathbf{z}_{s\pm}$ of the GGSZ analysis given in Eq. (2).

Their best-fit values are obtained by maximizing a combined likelihood function constructed as the product of partial likelihood P.D.F.s for GGSZ, GLW, and ADS measurements. The GGSZ likelihood function uses a 12-dimensional Gaussian P.D.F. with measurements $\mathbf{z}_{\pm}^{(*)}$ and $\mathbf{z}_{s\pm}$ and their covariance matrices for statistical, experimental systematic and amplitude-model uncertainties, and mean (expected) values $\bar{\mathbf{z}}_{\pm}^{(*)}$ and $\bar{\mathbf{z}}_{s\pm}$. Similarly, the GLW likelihood is formed as the product of four-dimensional Gaussian P.D.F.s for each B decay with measurements $A_{CP\pm}^{(*)}$, $A_{CP\pm}^{s}$, $R_{CP\pm}^{(*)}$, $R_{CP\pm}^{s}$, and their covariance matrices, and expected values given by Eqs. (6) and (7) after replacing the $\mathbf{z}_{\pm}^{(*)}$ and $\mathbf{z}_{s\pm}$ observables by the $\bar{\mathbf{z}}_{\pm}^{(*)}$ and $\bar{\mathbf{z}}_{s\pm}$ parameters. Finally, the ADS P.D.F. is built from the product of experimental likelihoods shown in Fig. 2. With this construction, GGSZ, GLW, and ADS observables are taken as uncorrelated. Similarly, the individual measurements are considered uncorrelated as the experimental uncertainties are dominated by the statistical component.

The combination requires external inputs for the D hadronic parameters r_D, δ_D, $r_{K\pi\pi^0}$, $\delta_{K\pi\pi^0}$, and $\kappa_{K\pi\pi^0}$. We assume Gaussian P.D.F.s for $r_D = 0.0575 \pm 0.0007$ [30] and $r_{K\pi\pi^0} = 0.0469 \pm 0.0011$ [47], while for the other three we adopt asymmetric Gaussian parametrizations based on the experimental likelihoods available either from world averages for $\delta_D = (202.0^{+9.9}_{-11.2})°$ [30] or from the CLEOc collaboration for $\delta_{K\pi\pi^0} = (47^{+14}_{-17})°$ and $\kappa_{K\pi\pi^0} = 0.84 \pm 0.07$ [48]. The values of δ_D and $\delta_{K\pi\pi^0}$ have been corrected for a shift of 180° in the definition of the phases between Refs. [23,24] and Refs. [30,48]. The correlations between r_D and δ_D, and between $\kappa_{K\pi\pi^0}$ and $\delta_{K\pi\pi^0}$, are small and have been neglected. All five external observables are assumed to be uncorrelated with the rest of the input observables.

The results for the combined CP-violating parameters $\bar{\mathbf{z}}_{\pm}^{(*)}$ and $\bar{\mathbf{z}}_{s\pm}$ are summarized in Table IV. Figure 3 shows comparisons of two-dimensional regions corresponding to one-, two-, and three-standard-deviation regions in the $\bar{\mathbf{z}}_{\pm}$, $\bar{\mathbf{z}}_{\pm}^{*}$, and $\bar{\mathbf{z}}_{s\pm}$ planes, including statistical and systematic uncertainties for GGSZ only, GGSZ and GLW methods combined, and the overall combination. These contours have been obtained using the likelihood ratio method, $-2\Delta\ln\mathcal{L} = s^2$, where s is the number of standard deviations, where $2\Delta\ln\mathcal{L}$ represents the variation of the combined log-likelihood with respect to its maximum value [47]. With this construction, the approximate confidence level (C.L.) in two dimensions for each pair of variables is 39.3%, 86.5%, and 98.9%. In these two-dimensional regions, the separation of the B^- and B^+ positions is equal to $2r_B|\sin\gamma|$, $2r_B^*|\sin\gamma|$, $2\kappa r_s|\sin\gamma|$ and is a measurement of direct CP violation, while the angle between the lines connecting the B^- and B^+ centers with the origin (0, 0) is equal to 2γ. Therefore, the net difference between $\bar{x}_+$ and $\bar{x}_-$ observed in Table IV and Fig. 3 is clear evidence for direct CP violation in $B^{\pm} \to DK^{\pm}$ decays.

TABLE IV. CP-violating complex parameters $\bar{\mathbf{z}}_{\pm}^{(*)} = \bar{x}_{\pm}^{(*)} + i\bar{y}_{\pm}^{(*)}$ and $\bar{\mathbf{z}}_{s\pm} = \bar{x}_{s\pm} + i\bar{y}_{s\pm}$ obtained from the combination of GGSZ, GLW, and ADS measurements. The first error is statistical (corresponding to $-2\Delta\ln\mathcal{L} = 1$), the second is the experimental systematic uncertainty including the systematic uncertainty associated to the GGSZ decay amplitude models.

	Real part (%)	Imaginary part (%)
$\bar{\mathbf{z}}_-$	$8.1 \pm 2.3 \pm 0.7$	$4.4 \pm 3.4 \pm 0.5$
$\bar{\mathbf{z}}_+$	$-9.3 \pm 2.2 \pm 0.3$	$-1.7 \pm 4.6 \pm 0.4$
$\bar{\mathbf{z}}_-^*$	$-7.0 \pm 3.6 \pm 1.1$	$-10.6 \pm 5.4 \pm 2.0$
$\bar{\mathbf{z}}_+^*$	$10.3 \pm 2.9 \pm 0.8$	$-1.4 \pm 8.3 \pm 2.5$
$\bar{\mathbf{z}}_{s-}$	$13.3 \pm 8.1 \pm 2.6$	$13.9 \pm 8.8 \pm 3.6$
$\bar{\mathbf{z}}_{s+}$	$-9.8 \pm 6.9 \pm 1.2$	$11.0 \pm 11.0 \pm 6.1$

In Fig. 3, we observe that when the information from the GLW measurements is included the constraints on the best-fit values of the parameters are improved. However, the constraints on $\bar{y}_{\pm}$ are poor due to the quadratic dependence and the fact that $r_B \ll 1$. This is the reason why the GLW method alone can hardly constrain γ. Similarly, Eq. (9) for the ADS method represents two circles in the $(\bar{x}_{\pm}, \bar{y}_{\pm})$ plane centered at $(r_B\cos\delta_D, r_D\sin\delta_D)$ and with radii $\sqrt{R_{\pm}}$. It is not possible to determine γ with only ADS observables because the true $(\bar{x}_{\pm}, \bar{y}_{\pm})$ points are distributed over two circles [49]. Therefore, while the GLW and ADS methods alone can hardly determine γ, when combined with the GGSZ measurements they help to improve significantly the constraints on the CP-violating parameters $\bar{\mathbf{z}}_{\pm}$, $\bar{\mathbf{z}}_{\pm}^{*}$, and $\bar{\mathbf{z}}_{s\pm}$.

V. INTERPRETATION OF RESULTS

In a second stage, we transform the combined $(\bar{x}_{\pm}, \bar{y}_{\pm})$, $(\bar{x}_{\pm}^{*}, \bar{y}_{\pm}^{*})$, and $(\bar{x}_{s\pm}, \bar{y}_{s\pm})$ measurements into the physically relevant quantities γ and the set of hadronic parameters $\mathbf{u} \equiv (r_B, r_B^*, \kappa r_s, \delta_B, \delta_B^*, \delta_s)$. We adopt a frequentist procedure [50] to obtain one-dimensional confidence intervals of well-defined C.L. that takes into account non-Gaussian effects due to the nonlinearity of the relations between the observables and physical quantities. This procedure is identical to that used in Refs. [17,18,20,22,23].

We define a χ^2 function as

$$\chi^2(\gamma, \mathbf{u}) \equiv -2\Delta\ln\mathcal{L}(\gamma, \mathbf{u}) \equiv -2[\ln\mathcal{L}(\gamma, \mathbf{u}) - \ln\mathcal{L}_{\max}], \tag{11}$$

where $2\Delta\ln\mathcal{L}(\gamma, \mathbf{u})$ is the variation of the combined log-likelihood with respect to its maximum value, with the $\bar{\mathbf{z}}_{\pm}^{(*)}$

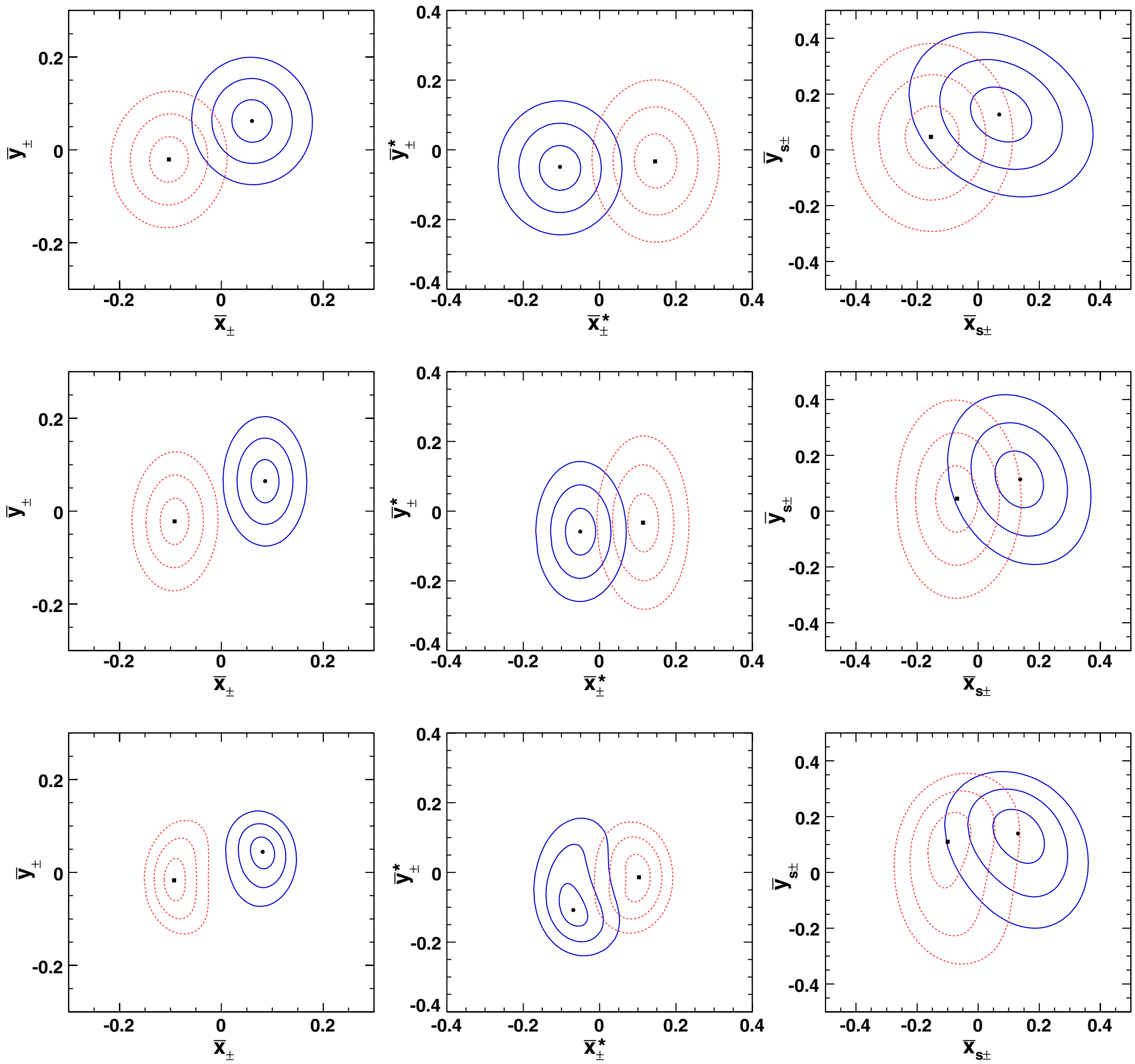

FIG. 3 (color online). Two-dimensional $-2\Delta \ln \mathcal{L} = s^2$ contours (up to three standard deviations, i.e., $s = 1, 2, 3$) in the $\bar{\mathbf{z}}_{\pm}$ (left column), $\bar{\mathbf{z}}^{*}_{\pm}$ (center column), and $\bar{\mathbf{z}}_{s\pm}$ (right column) planes, for the GGSZ measurement only (top row), the GGSZ and GLW combination (middle row), and the GGSZ, GLW, and ADS combination (bottom row). The solid (blue) and dashed (red) lines correspond to B^- and B^+ decays.

and $\bar{\mathbf{z}}_{s\pm}$ expected values written in terms of γ and $\mathbf{u}$, i.e., replacing $\bar{\mathbf{z}}^{(*)}_{\pm}$ and $\bar{\mathbf{z}}_{s\pm}$ by $r^{(*)}_B e^{i(\delta^{(*)}_B \pm \gamma)}$ and $\kappa r_s e^{i(\delta_s \pm \gamma)}$, respectively. To evaluate the C.L. of a certain parameter (for example γ) at a given value (γ_0), we consider the value of the χ^2 function at the new minimum, $\chi^2_{\rm min}(\gamma_0, \mathbf{u}_0)$, satisfying $\Delta\chi^2(\gamma_0) = \chi^2_{\rm min}(\gamma_0, \mathbf{u}_0) - \chi^2_{\rm min} \geq 0$. In a purely Gaussian situation, the C.L. is given by the probability that $\Delta\chi^2(\gamma_0)$ is exceeded for a χ^2 distribution with one degree of freedom, $1 - \text{C.L.} = \text{Prob}[\Delta\chi^2(\gamma_0); \nu = 1]$, where $\text{Prob}[\Delta\chi^2(\gamma_0); \nu = 1]$ is the corresponding cumulative distribution function (this approach is later referred to as "Prob method") [47]. In a non-Gaussian situation one has to consider $\Delta\chi^2(\gamma_0)$ as a test statistic, and rely on a Monte Carlo simulation to obtain its expected distribution. This Monte Carlo simulation is performed by generating more than 10^9 samples (sets of the 39 GGSZ, GLW, ADS, and *D*-decay observable values), using the combined likelihood evaluated at values $(\gamma_0, \mathbf{u}_0)$, i.e., $\mathcal{L}(\gamma_0, \mathbf{u}_0)$. The confidence level C.L. is determined from the fraction of experiments for which $\Delta\chi'^2(\gamma_0) > \Delta\chi^2(\gamma_0)$, where $\Delta\chi'^2(\gamma_0) = \chi'^2(\gamma_0, \mathbf{u}'_0) - \chi'^2_{\rm min}$ for each simulated experiment is determined as in the case of the actual data sample. We adopt the Monte Carlo simulation method as baseline to determine the C.L., and allow $0 \leq r^{(*)}_B, \kappa r_s \leq 1$ and $-180° \leq \gamma, \delta^{(*)}_B, \delta_s \leq 180°$.

Figure 4 illustrates $1 - \text{C.L.}$ as a function of γ, $r^{(*)}_B$, κr_s, $\delta^{(*)}_B$ and δ_s, for each of the three *B*-decay channels separately and, in the case of γ, their combination. The combination has the same twofold ambiguity in the weak and strong phases as that of the GGSZ method,

$(\gamma; \delta_B^{(*)}, \delta_s) \to (\gamma + 180°; \delta_B^{(*)} + 180°, \delta_s + 180°)$. From these distributions, we extract one- and two-standard-deviation intervals as the sets of values for which $1 - \mathrm{C.L.}$ is greater than 31.73% and 4.55%, respectively, as summarized in Table V. When comparing these intervals to those obtained with the GGSZ method only, also shown in Table V, we observe that the combination helps to improve the constraints on $r_B^{(*)}$ and κr_s, but not those on γ. To assess the impact of the GLW and ADS observables in the determination of γ, we compare $1 - \mathrm{C.L.}$ as a function of $r_B^{(*)}$ and γ for all B-decay channels combined using the GGSZ method alone, the combination with the GLW measurements, and the global combination, as shown in Fig. 5. While the constraints on r_B are clearly improved at the one- and two-standard-deviation level, and to a lesser extent on r_B^*, their best (central) values move towards slightly lower values. Since the uncertainty on γ scales approximately as $1/r_B^{(*)}$, the constraints on γ at 68.3% and 95.4% C.L. do not improve, in spite of the tighter constraints on the combined measurements shown in Fig. 3. However, adding GLW and ADS information reduces the confidence intervals for smaller $1 - \mathrm{C.L.}$, as a consequence of the more Gaussian behavior when the significance of excluding $r_B^{(*)} = 0$ increases. Thus, for example, in the region close to four standard deviations, the GGSZ method alone does not constrain γ, while the combination is able to exclude large regions.

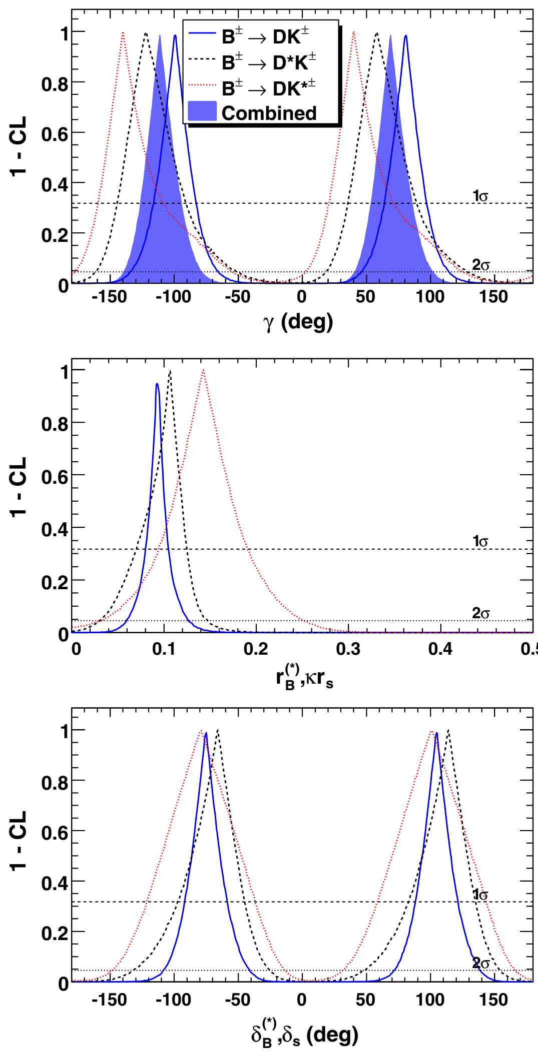

FIG. 4 (color online). $1 - \mathrm{C.L.}$ distributions for the combination of the GGSZ, GLW, and ADS methods as a function of γ (top), $r_B^{(*)}$, and κr_s (middle), and $\delta_B^{(*)}$, δ_s (bottom), including statistical and systematic uncertainties, for $B^\pm \to DK^\pm$, $B^\pm \to D^*K^\pm$, and $B^\pm \to DK^{*\pm}$ decays. The combination of all the B-decay channels is also shown for γ. The dashed (dotted) horizontal line corresponds to the one- (two-) standard-deviation C.L.

TABLE V. 68.3% and 95.5% one-dimensional C.L. regions, equivalent to one- and two-standard-deviation intervals, for γ, $\delta_B^{(*)}$, δ_s, $r_B^{(*)}$, κr_s, including all sources of uncertainty, obtained from the combination of GGSZ, GLW, and ADS measurements. The combined results are compared to those obtained using the GGSZ measurements only, taken from Ref. [17]. The results for γ, $\delta_B^{(*)}$, and δ_s are given modulo a 180° phase.

	68.3% C.L.		95.5% C.L.	
Parameter	Combination	GGSZ	Combination	GGSZ
γ (°)	69^{+17}_{-16}	68^{+15}_{-14}	[41, 102]	[39, 98]
r_B (%)	$9.2^{+1.3}_{-1.2}$	9.6 ± 2.9	[6.0, 12.6]	[3.7, 15.5]
r_B^* (%)	$10.6^{+1.9}_{-3.6}$	$13.3^{+4.2}_{-3.9}$	[3.0, 14.7]	[4.9, 21.5]
κr_s (%)	$14.3^{+4.8}_{-4.9}$	$14.9^{+6.6}_{-6.2}$	[3.3, 25.1]	<28.0
δ_B (°)	105^{+16}_{-17}	119^{+19}_{-20}	[72, 139]	[75, 157]
δ_B^* (°)	-66^{+21}_{-31}	-82 ± 21	[−132, −26]	[−124, −38]
δ_s (°)	101 ± 43	111 ± 32	[32, 166]	[42, 178]

The significance of direct CP violation is obtained by evaluating $1 - \mathrm{C.L.}$ for the most probable CP conserving point, i.e., the set of hadronic parameters $\mathbf{u}$ with $\gamma = 0$. Including statistical and systematic uncertainties, we obtain $1 - \mathrm{C.L.} = 3.4 \times 10^{-7}$, 2.5×10^{-3}, and 3.6×10^{-2}, corresponding to 5.1, 3.0, and 2.1 standard deviations, for $B^\pm \to DK^\pm$, $B^\pm \to D^*K^\pm$, and $B^\pm \to DK^{*\pm}$ decays, respectively. For the combination of the three decay modes we obtain $1 - \mathrm{C.L.} = 3.1 \times 10^{-9}$, corresponding to 5.9 standard deviations. For comparison, the corresponding significances with the GGSZ method alone are 2.9, 2.8, 1.5, and 4.0 standard deviations [51], while with the GGSZ and GLW combination they are 4.8, 2.7, 1.8, and 5.4, respectively.

The frequentist procedure used to obtain γ and the hadronic parameters $\mathbf{u}$ is not guaranteed to have perfect coverage, especially for low values of $r_B^{(*)}$, r_s. This is due to the treatment of nuisance parameters [50]. Instead of scanning the entire parameter space defined by γ and $\mathbf{u}$ (seven dimensions), we perform one-dimensional scans, in which, during MC generation, the nuisance parameters are set to their reoptimized best-fit values at each scan point. In order to evaluate the coverage properties of our procedure, we generate more than 10^9 samples with true values of $(\gamma, \mathbf{u})$

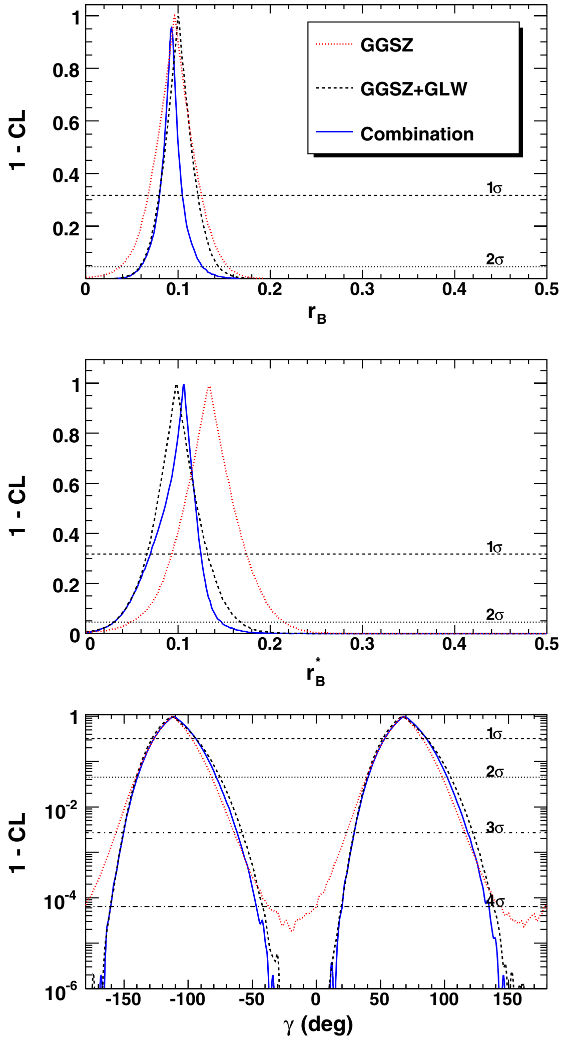

FIG. 5 (color online). Comparison of $1 - \mathrm{C.L.}$ as a function of r_B (top), r_B^* (middle), and γ (bottom) for all B-decay channels combined with the GGSZ method only, the combination with the GLW measurements, and the global combination, including statistical and systematic uncertainties. The horizontal lines represent the one-, two-, three-, and four-standard-deviation C.L.

set to their best-fit values, $(\gamma_{\mathrm{best}}, \mathbf{u}_{\mathrm{best}})$, as given in Table V. For each generated experiment, we determine $1 - \mathrm{C.L.}'$ at $\gamma_0 = \gamma_{\mathrm{best}}$, as done previously with the actual data sample using the Monte Carlo simulation method. The statistical coverage α, defined as the probability for the true value of γ (γ_0) to be inside the given $1 - \mathrm{C.L.}$ interval, is evaluated as the fraction of experiments with $1 - \mathrm{C.L.}'$ larger than $1 - \mathrm{C.L.}$ We obtain $\alpha = 0.679 \pm 0.005$ (0.955 ± 0.002) for the combination, and $\alpha = 0.670 \pm 0.005$ (0.950 ± 0.002) for the GGSZ method alone, for $\mathrm{C.L.} = 0.683$ (0.954), respectively. For comparison purposes, the corresponding values using the Prob method are $\alpha = 0.641 \pm 0.005$ (0.941 ± 0.003) and $\alpha = 0.609 \pm 0.005$ (0.920 ± 0.003). While the Prob method tends to underestimate the confidence intervals, the Monte Carlo simulation approach provides intervals with correct coverage, especially for the combination where the magnitude ratios between the suppressed and favored decays have more stringent constraints.

VI. SUMMARY

In summary, using up to 474×10^6 $B\bar{B}$ decays recorded by the *BABAR* detector, we have presented a combined measurement of the CP-violating ratios between the $b \to u\bar{c}s$ and $b \to c\bar{u}s$ amplitudes in processes $B^\pm \to D^{(*)}K^\pm$ and $B^\pm \to DK^{*\pm}$. The combination procedure maximizes the information provided by the most sensitive γ measurements and analysis techniques that exploit a large number of D-decay final states, including three-body self-conjugate, CP, and doubly-Cabibbo-suppressed states, resulting in the most precise measurement of these ratios. From the measurements of these ratios we determine $\gamma = (69^{+17}_{-16})°$ modulo 180°, where the total uncertainty is dominated by the statistical component, with the experimental and amplitude-model systematic uncertainties amounting to $\pm 4°$. We also derive the most precise determinations of the magnitude ratios $r_B^{(*)}$ and κr_s. The two-standard-deviation region for γ is $41° < \gamma < 102°$. The combined significance of $\gamma \neq 0$ is $1 - \mathrm{C.L.} = 3.1 \times 10^{-9}$, corresponding to 5.9 standard deviations, meaning observation of direct CP violation in the measurement of γ. These results supersede our previous constraints based on the GGSZ, GLW, and ADS analyses of charged B decays [17–21,23,24], and are consistent with the range of values implied by other experiments [36–44].

ACKNOWLEDGMENTS

We are grateful for the extraordinary contributions of our PEP-II colleagues in achieving the excellent luminosity and machine conditions that have made this work possible. The success of this project also relies critically on the expertise and dedication of the computing organizations that support *BABAR*. The collaborating institutions wish to thank SLAC for its support and the kind hospitality extended to them. This work is supported by the US Department of Energy and National Science Foundation, the Natural Sciences and Engineering Research Council (Canada), the Commissariat à l'Energie Atomique and Institut National de Physique Nucléaire et de Physique des Particules (France), the Bundesministerium für Bildung und Forschung and Deutsche Forschungsgemeinschaft (Germany), the Istituto Nazionale di Fisica Nucleare (Italy), the Foundation for Fundamental Research on Matter (The Netherlands), the Research Council of Norway, the Ministry of Education and Science of the Russian Federation, Ministerio de Economía y Competitividad (Spain), and the Science and Technology Facilities Council (United Kingdom). Individuals have received support from the Marie-Curie IEF program (European Union) and the A. P. Sloan Foundation (USA).

[1] N. Cabibbo, Phys. Rev. Lett. **10**, 531 (1963); M. Kobayashi and T. Maskawa, Prog. Theor. Phys. **49**, 652 (1973).
[2] J. Charles, A. Höcker, H. Lacker, S. Laplace, F. R. Diberder, J. Malclés, J. Ocariz, M. Pivk, and L. Roos, Eur. Phys. J. C **41**, 1 (2005) and updates at http://ckmfitter.in2p3.fr/; M. Bona *et al.*, J. High Energy Phys. 03 (2008) 049 and updates at http://www.utfit.org/.
[3] J. Zupan, arXiv:1101.0134.
[4] R. Fleischer, Phys. Lett. B **459**, 306 (1999).
[5] M. Gronau, D. Pirjol, A. Soni, and J. Zupan, Phys. Rev. D **75**, 014002 (2007).
[6] M. Ciuchini, M. Pierini, and L. Silvestrini, Phys. Rev. D **74**, 051301 (2006).
[7] A. Giri, Y. Grossman, A. Soffer, and J. Zupan, Phys. Rev. D **68**, 054018 (2003).
[8] M. Gronau and D. London, Phys. Lett. B **253**, 483 (1991); M. Gronau and D. Wyler, Phys. Lett. B **265**, 172 (1991).
[9] D. Atwood, I. Dunietz, and A. Soni, Phys. Rev. Lett. **78**, 3257 (1997); Phys. Rev. D **63**, 036005 (2001).
[10] Charge conjugate modes are implicitly included unless otherwise stated.
[11] T. E. Browder, K. Honscheid, and D. Pedrini, Annu. Rev. Nucl. Part. Sci. **46**, 395 (1996).
[12] M. Gronau, Phys. Lett. B **557**, 198 (2003).
[13] J. P. Lees *et al.* (*BABAR* Collaboration), Phys. Rev. D **84**, 112007 (2011).
[14] K. Trabelsi (Belle Collaboration), arXiv:1301.2033.
[15] R. Aaij *et al.* (LHCb Collaboration), Report No. CERN-LHCb-CONF-2012-032.
[16] B. Aubert *et al.* (*BABAR* Collaboration), Nucl. Instrum. Methods Phys. Res., Sect. A **479**, 1 (2002).
[17] P. del Amo Sanchez *et al.* (*BABAR* Collaboration), Phys. Rev. Lett. **105**, 121801 (2010).
[18] B. Aubert *et al.* (*BABAR* Collaboration), Phys. Rev. D **78**, 034023 (2008).
[19] B. Aubert *et al.* (*BABAR* Collaboration), Phys. Rev. Lett. **95**, 121802 (2005).
[20] P. del Amo Sanchez *et al.* (*BABAR* Collaboration), Phys. Rev. D **82**, 072004 (2010).
[21] B. Aubert *et al.* (*BABAR* Collaboration), Phys. Rev. D **78**, 092002 (2008).
[22] B. Aubert *et al.* (*BABAR* Collaboration), Phys. Rev. D **80**, 092001 (2009).
[23] P. del Amo Sanchez *et al.* (*BABAR* Collaboration), Phys. Rev. D **82**, 072006 (2010).
[24] J. P. Lees *et al.* (*BABAR* Collaboration), Phys. Rev. D **84**, 012002 (2011).
[25] B. Aubert *et al.* (*BABAR* Collaboration), Phys. Rev. Lett. **99**, 251801 (2007).
[26] B. Aubert *et al.* (*BABAR* Collaboration), Phys. Rev. D **79**, 072003 (2009).
[27] B. Aubert *et al.* (*BABAR* Collaboration), Phys. Rev. D **80**, 031102(R) (2009).
[28] B. Aubert *et al.* (*BABAR* Collaboration), Phys. Rev. D **71**, 112003 (2005).
[29] B. Aubert *et al.* (*BABAR* Collaboration), Phys. Rev. D **73**, 111101(R) (2006).
[30] Y. Amhis *et al.* (Heavy Flavor Averaging Group Collaboration), arXiv:1207.1158.
[31] Y. Grossman, A. Soffer, and J. Zupan, Phys. Rev. D **72**, 031501 (2005).
[32] There is a misprint in the analogous decay rate written in Ref. [17].
[33] A. Bondar and T. Gershon, Phys. Rev. D **70**, 091503 (2004).
[34] P. del Amo Sanchez *et al.* (*BABAR* Collaboration), Phys. Rev. Lett. **105**, 081803 (2010).
[35] A. Bondar and A. Poluektov, Eur. Phys. J. C **47**, 347 (2006); **55**, 51 (2008).
[36] H. Aihara *et al.* (Belle Collaboration), Phys. Rev. D **85**, 112014 (2012).
[37] A. Poluektov *et al.* (Belle Collaboration), Phys. Rev. D **81**, 112002 (2010).
[38] R. Aaij *et al.* (LHCb Collaboration), Phys. Lett. B **718**, 43 (2012).
[39] K. Abe *et al.* (Belle Collaboration), Phys. Rev. D **73**, 051106 (2006); Report No. BELLE-CONF-1112.
[40] T. Aaltonen *et al.* (CDF Collaboration), Phys. Rev. D **81**, 031105 (2010).
[41] R. Aaij *et al.* (LHCb Collaboration), Phys. Lett. B **712**, 203 (2012); **713**, 351(E) (2012).
[42] Y. Horii *et al.* (Belle Collaboration), Phys. Rev. Lett. **106**, 231803 (2011).
[43] K. Negishi *et al.* (Belle Collaboration), Phys. Rev. D **86**, 011101 (2012).
[44] T. Aaltonen *et al.* (CDF Collaboration), Phys. Rev. D **84**, 091504 (2011).
[45] I. Dunietz, Phys. Lett. B **427**, 179 (1998).
[46] B. Aubert *et al.* (*BABAR* Collaboration), Phys. Rev. D **77**, 071102(R) (2008).
[47] K. Nakamura *et al.* (Particle Data Group), J. Phys. G **37**, 075021 (2010).
[48] N. Lowrey *et al.* (CLEOc Collaboration), Phys. Rev. D **80**, 031105(R) (2009).
[49] M. Rama, Proc. Sci., FPCP2009 (2009) 003.
[50] B. Sen, M. Walker, and M. Woodroofe, Statistica Sinica **19**, 301 (2009).
[51] These values supersede those given in Ref. [17], which were slightly underestimated.